Single-molecule fluorescence autocorrelation experiments on pentacene

Brouwer, A. C. J.; Köhler, J.; van Oijen, A. M. ; Groenen, E. J. J.; Schmidt, J.

Published in:
Journal of Chemical Physics

DOI:
10.1063/1.478837

Publication date:
1999

Single-molecule fluorescence autocorrelation experiments on pentacene: The dependence of intersystem crossing on isotopic composition

A. C. J. Brouwer, J. Köhler, A. M. van Oijen, E. J. J. Groenen, and J. Schmidt

Citation: J. Chem. Phys. **110**, 9151 (1999); doi: 10.1063/1.478837
View online: https://doi.org/10.1063/1.478837
View Table of Contents: http://aip.scitation.org/toc/jcp/110/18
Published by the American Institute of Physics

Single-molecule fluorescence autocorrelation experiments on pentacene: The dependence of intersystem crossing on isotopic composition

A. C. J. Brouwer, J. Köhler, A. M. van Oijen, E. J. J. Groenen, and J. Schmidt
Centre for the Study of Excited States of Molecules, Huygens Laboratory, University of Leiden, P.O. Box 9504, 2300 RA Leiden, The Netherlands

(Received 8 December 1998; accepted 16 February 1999)

Single pentacene molecules containing ^{13}C or ^{1}H in a pentacene-d_{14} doped *p*-terphenyl crystal have been studied by fluorescence autocorrelation. The triplet dynamics has been analyzed and a systematic dependence of the $S_1 \rightarrow T_1$ intersystem crossing rate on isotopic composition was found. This variation is discussed in terms of a modulation of the near resonance of the first excited singlet state S_1 and vibrational levels of an intermediating triplet state T_3 which results from the distinct isotope dependence of the zero-point energy of both electronic states. © *1999 American Institute of Physics.* [S0021-9606(99)01518-4]

I. INTRODUCTION

The development of spectroscopy on single molecules in solid matrices has enabled novel experiments and allowed the discrimination of subtle effects as reviewed in Refs. 1–4. For example, the fluorescence signal of a single molecule, as opposed to ensemble fluorescence, contains information on the evolution of the molecular wave function through the quantum states accessible under optical excitation. This information can be exploited to determine the intersystem crossing rates between the singlet and triplet manifold either by recording the intensity autocorrelation of a molecule's fluorescence[5] or by directly timing the singlet and triplet residence of a molecule through the presence or absence of fluorescence.[6,7] In previous work we have explored the effects of isotopic composition of pentacene through optical excitation spectroscopy and magnetic resonance.[8,9] Here we extend this work and refine the involved techniques so as to examine the dependence of the intersystem crossing (ISC) of pentacene on its isotopic composition.

Pentacene substitutionally occupies one of four low-temperature crystal sites in the *p*-terphenyl host crystal giving rise to four spectral origins in the $S_1 \leftarrow S_0$ excitation spectrum labeled O_1–O_4 in order of increasing frequency. The low ISC for the O_1 and O_2 sites makes them suited to single-molecule spectroscopy. In fact, pentacene in *p*-terphenyl was the first system used in single-molecule spectroscopy.[10,11] The isotope shifts of the $S_1 \leftarrow S_0$ $0-0$ transition as observed in the spectrum shown in Fig. 1 result from the dependence of the zero-point energy on isotopic composition and electronic state. Clearly, many isotopic isomers are present, at a low relative concentration, in the used batch of deuterated pentacene. These isotopomers result from a small residue of ^{1}H left after deuteration so that no additional synthesis was required to obtain them. By combining frequency and spatial selectivity it proves possible to select single molecules for a wide range of these species so as to study their intersystem crossing on an equal footing irrespective of the apparent vast differences in concentration.

Our interest is motivated by the remarkable sensitivity of the pentacene $S_1 \rightarrow T_1$ ISC to the (site of the) host matrix. When embedded in *p*-terphenyl at liquid-helium temperatures, the O_3 and O_4 sites have rates exceeding those of the O_1 and O_2 sites by two orders of magnitude.[12,13] When increasing the temperature, the O_1 and O_2 ISC rates were observed to converge to those of O_3 and O_4.[13,14] For pentacene in benzoic acid at 1.6 K, the ISC was shown to be dominated by a near-resonance of the first excited singlet state S_1 and a vibrational level of a higher triplet state. A level crossing was observed when shifting the triplet sublevels by applying a strong magnetic field.[15]

At a microsecond time scale, the fluorescence of a pentacene molecule exhibits a phenomenon called photon bunching.[11] This is due to the fact that the repeated excitation to the S_1 state followed by the emission of a fluorescence photon is interrupted when the molecule crosses over to the triplet state thus leading to bunches of photons separated by dark periods. It was shown by Bernard *et al.* that photon bunching can be used to determine intersystem crossing rates.[5] In this study we deploy their method to determine the dependence of the ISC on isotopic composition. We will show how the measured changes in ISC can be interpreted in terms of electronic structure differences between S_1 and a mediating triplet state. Isotope shifts are found to be crucial because they tune the near resonance of S_1 and vibrational levels of the triplet.

II. EXPERIMENT

A. Instrumentation

A single-mode dye laser (Coherent, 599-21), intensity stabilized using an electro-optical modulator (EOM, ConOptics 370), served as excitation light source. The limited dynamic range of the EOM was extended using a variable grey filter. The light is delivered via a polarization preserving single-mode fiber to a confocal detection arrangement (see Fig. 2). Neutral density filters placed in the intensity stabilization feedback path allowed a calibrated change of the excitation intensity in doubling steps over a range of three decades. A fine lateral optimization of the detection volume

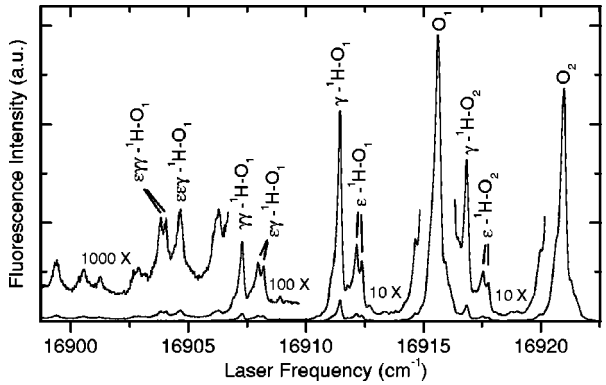

FIG. 1. Excitation spectrum of pentacene-d_{14} doped p-terphenyl-d_{14} near the O_1 and O_2 sites. Parts of the spectrum are scaled to better show the weak redshifted satellites caused by various isotopic isomers of not fully deuterated pentacene. The labels indicate the position of ^{1}H (see Fig. 6) as well as the associated site.

could be achieved by tilting a telecentrically placed motorized scan mirror. Experiments were performed at a temperature of 2 K with the sample mounted inside a helium bath cryostat. A translation mechanism allows movement of the sample perpendicular to the excitation cone over a range of 2 mm. The depth of the excitation focus was tuned by moving the objective lens towards or away from the sample. The focal volume is roughly 2 μm^3. After separation using a dichroic and long-pass filter, the fluorescence photons were detected using an avalanche photodiode (EG&G SPCM-200-PQ). Photon counts were read by a multichannel scaling card (EG&G 923 MCS-plus) configured for continuous circularly buffered counting. Autocorrelation measurements were performed by applying a highly optimized algorithm to this incoming stream of counting values at a time resolution of 2 μs.

The experiments were controlled and processed through a fully integrated computerized data acquisition system. The laser scan range was linearized and calibrated in relative units by reference to a Fabry–Perot etalon. Wide excitation spectra were obtained by recording overlapping ($<$30 GHz) single-mode sweeps and combining these using the frequency specific excitation pattern of an iodine cell recorded in parallel. The corresponding composite iodine spectrum allowed absolute calibration ($\pm$0.002 cm^{-1}) by reference to tabulated iodine lines.[16,17] For random positioning of the laser to a particular frequency or relative to a previously recorded excitation spectrum, a current small iodine excitation sweep is matched to a preconstructed composite iodine spectrum covering the spectral range of interest, a method that works even when tabulated iodine lines are sparse. While averaging subsequent laser sweeps for excitation spectra, the laser drift was compensated for to within roughly 1 MHz using the iodine pattern recorded simultaneously. While performing measurements on a single molecule (fixed laser frequency), the laser drift was removed by periodically interrupting the measurement and making a small excitation sweep around the molecule after which the laser was retuned to the center of its absorption. For improved accuracy, power broadening is circumvented by switching the laser to low intensity during such a compensation sweep.

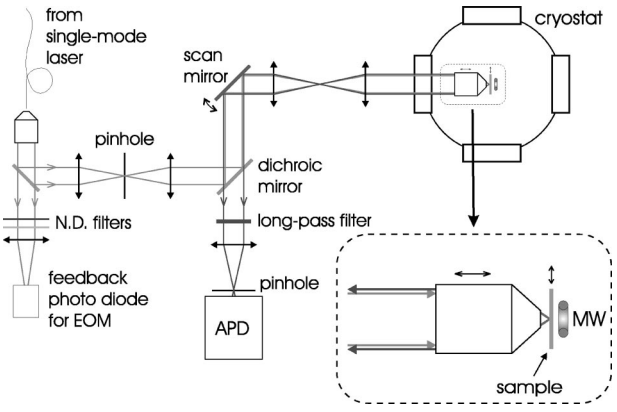

FIG. 2. Confocal detection arrangement.

While recording fluorescence-detected magnetic-resonance (FDMR) spectra the sample was exposed to microwaves by way of a small grounded loop close to the sample. The microwaves were generated by a sweep oscillator (HP 8350 B) and amplified. Magnetic resonance was detected directly as a decrease in fluorescence. The microwave frequency range was calibrated using a frequency counter (EIP 371). During averaging, the drift was compensated to 10 kHz rms by periodically interrupting the microwave sweeps for a frequency reading.

Excitation and FDMR spectra were recorded at an excess spectral resolution. An optimal tradeoff between spectral resolution and intensity noise was made after the measurements by fitting cubic splines to the data. The ''bandwidth'' of the splines was chosen such that the narrowest spectral features could still be well represented.

B. Sample preparation

The spectrum shown in Fig. 1 was recorded for a deuterated p-terphenyl crystal containing a relatively high pentacene concentration so that even isotopomeric species with a very low abundance could be resolved. The same batch of mostly deuterated pentacene was used at a much lower concentration for the experiments described in this article but instead of deuterated p-terphenyl, natural abundance p-terphenyl served as a host matrix. This explains the slight difference in the frequencies of the $S_1 \leftarrow S_0$ 0–0 transition of the spectral sites in Fig. 1 compared to the other spectra.

Thin, doped crystal flakes were grown by cosublimation of pentacene and zone-refined p-terphenyl. The sublimation temperatures were independently stabilized to control the growth rate and pentacene concentration. Most experiments were performed on a flake sublimed at 170 °C for p-terphenyl and 60 °C for pentacene-d_{14} resulting in a pentacene concentration of roughly 10^{-8} mol/mol. Molecules belonging to the two most abundant isotopomeric species (those fully deuterated or protonated in the γ position only) were selected from a crystal sublimed at 180 °C/50 °C resulting in a somewhat lower pentacene concentration which made it easier to select isolated molecules.

The chosen crystals had a very small degree of inhomogeneous broadening [roughly 1 GHz full width at half maxi-

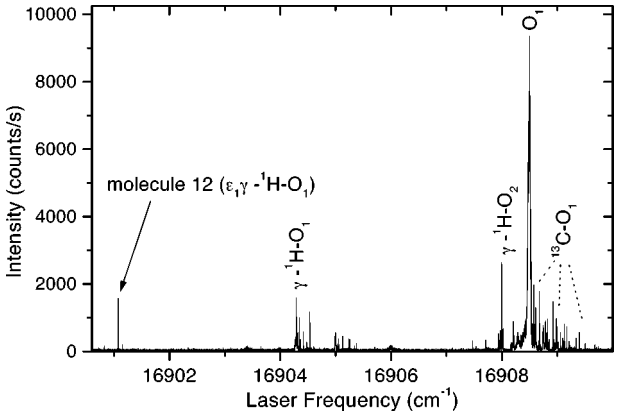

FIG. 3. In-focus excitation spectrum of the pentacene-d_{14} doped *p*-terphenyl crystal from which nearly all examined molecules were selected. Individual molecules appear as spikes. Evidently, for most isotopomer species only a couple or less molecules are in focus.

TABLE I. Isotope shifts of the singly substituted satellite bands relative to the all-deutero O_1 and O_2 sites.

	O_1 site	O_2 site
Assignment	Shift (cm^{-1})	Shift (cm^{-1})
α_2-^{1}H	−0.308	−0.326
β_1-^{1}H	−0.756	−0.774
β_2-^{1}H	−0.990	−1.027
ε_1-^{1}H	−3.252	−3.213
ε_2-^{1}H	−3.487	−3.447
γ-^{1}H	−4.194	−4.128
ζ-^{13}C	0.099	0.090
α,δ-^{13}C	0.299	0.308
ε-^{13}C	0.484	0.485
γ-^{13}C	0.619	0.609

mum (FWHM)]. This is a prerequisite since it has been shown that for crystals with a large degree of inhomogeneous broadening a wide spread of the intersystem crossing rates for individual molecules results[18] so that any isotopomer specific effects would be hard to resolve. Furthermore, a smaller degree of inhomogenous broadening diminishes overlap between the isotopomer bands causing the isotope shift to become a more accurate selection criterion.

As will be explained later, determining intersystem crossing rates requires autocorrelation measurements over a wide range of excitation intensities. At high excitation intensity, power broadening (up to a couple of hundred MHz) and an increase in the background relative to the fluorescence of the saturated molecule occurs so that the molecule is required to be spectrally very well isolated. For this reason the pentacene concentration was chosen sufficiently low to make sure that for a range of isotopomers at most a couple of molecules were present within a focal volume (see Fig. 3). To nevertheless find single molecules for rare species, different spots across the crystal were probed for as long as it took to stumble over a molecule. An added advantage of this method is that for most isotopomeric species the spectral density of molecules was sufficiently low to allow selection of a molecule from the middle of the corresponding inhomogenous range thus decreasing the odds of selecting a molecule from another site or isotopic composition in an exceptional environment.

C. Experimental protocol

A sizable set of molecules belonging to various isotopomeric species were examined in this study. Instead of detailing how each molecule was selected and identified, we limit ourselves to describing the general protocol used.

Previously we have shown that the isotope shifts of ^{13}C-containing pentacene isomers present in natural abundance and ^{1}H isomers resulting from incomplete deuteration obey a sum rule such that the shift for an isotopomer containing multiple ^{13}C's or ^{1}H's can be predicted, to a high degree of accuracy, by summing the shifts of the corresponding singly substituted isotopomers.[8,9] Thus, after deciding upon the isotopomeric species and site of the molecule to be studied, the expected isotope shift can either be looked up (see Table I) or calculated using this sum rule. Subsequently, the precise center frequency of the corresponding all-deutero site at the current sample position is determined by recording an excitation spectrum. Adding the shift to the site frequency gives the position of the center of the isotopomer band. Next, an excitation scan a few GHz wide around the band center is repeatedly performed while the sample is slowly translated until a molecule appears in the spectrum. If the sample had to be translated by a large amount before the molecule was found, the center frequency of the related all-deutero site is verified once more since it shifts slightly (less than 1.5 GHz) over the probed range of sample positions.

Having found a molecule, the focal volume is centered on it by translating the objective lens and fine tuning the scan mirror until the detected fluorescence at nonsaturating excitation power is maximized. Next, high-resolution excitation spectra of the molecule are averaged at low and high excitation power. If the low-power line shape is symmetric and has a width corresponding to the lifetime limited value plus a small fixed instrumental contribution, the molecule can be assumed to be spectrally stable and isolated. The high power spectrum serves to check whether the fluorescence background does not swamp the fluorescence of the saturated molecule and whether the molecule remains spectrally isolated at excitation intensities that cause significant power broadening (up to a couple of hundred MHz FWHM). If the results are satisfactory, the laser frequency is stabilized to the center of the molecule's absorption resulting in a fluorescence signal stemming solely from that molecule.

To verify the identity of the molecule, FDMR spectra of the $T_x - T_z$ transition are recorded at a couple of microwave powers (see Sec. III B). If the line shape is as expected for the desired isotopomer and the zero-field splitting matches that of the site the molecule is supposed to belong to, the identity of the molecule is confirmed and the correlation measurements (see Sec. IV) can commence. At each excitation power, the autocorrelation histogram is accumulated to an accuracy that allows a proper exponential fit. The series of correlation measurements is repeated as allowed by the avail-

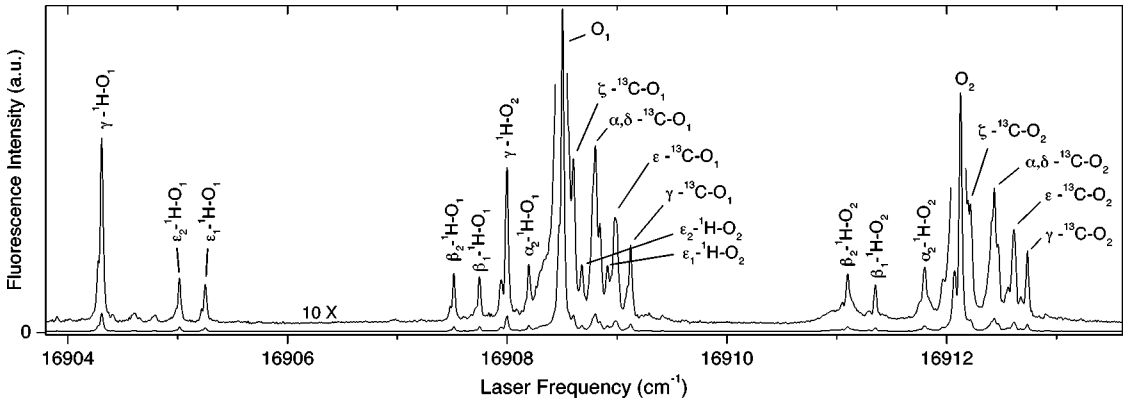

FIG. 4. Out-of-focus excitation spectrum of the pentacene-d_{14} doped *p*-terphenyl crystal from which nearly all examined molecules were selected. Both ^{13}C and ^{1}H satellites are resolved.

ability of liquid helium so as to gauge reproducibility and improve the accuracy of the overall fit.

III. OPTICAL SHIFTS AND MAGNETIC RESONANCE OF ISOTOPIC ISOMERS

The main thrust of this article concerns the measurement of the intersystem crossing rates of pentacene isotopomers and their interpretation. In order to enable the selection of molecules belonging to particular isotopomer species, intermediate experiments have to be carried out as will be discussed in this section. Specifically, excitation spectra serve the determination of S_0-S_1 isotope shifts as well as the optical selection of single molecules. Fluorescence-detected magnetic resonance is used to assign isotope shifted sidebands and verify the composition and site of selected single molecules.

A. Excitation spectra and isotope shifts

Figure 4 shows an excitation spectrum of pentacene-d_{14} in *p*-terphenyl covering the range that includes all singly substituted isotopomer satellites of the O_1 and O_2 spectral sites. The spectrum was recorded of the same sample from which nearly all molecules were selected. Statistical fine structure due to the low concentration was avoided by tuning the objective lens out of focus and reducing the spatial selectivity of the detection optics. The spectrum is somewhat complicated by the presence of smooth, slightly redshifted sidebands (see Fig. 5) caused by spectrally diffusing molecules. Since the various isotopomers share the same distribution of local environments and have virtually identical photophysical properties, the inhomogeneous broadening and sidebands are replicated for all isotopomer satellites of a site. For O_2, relatively many spectrally diffusing molecules appear at a redshift of roughly 1 cm^{-1} which explains the broad intensity below satellites β_1 and β_2. With these provisos in mind it can be seen that O_1 and O_2 have nearly identical satellite patterns which partially overlap. The assignment of the ^{13}C satellites to the blue of either site was made in analogy with the assignment in Ref. 8 for pentacene-h_{14}. Because of the lowered vibrational frequencies for pentacene-d_{14}, the pattern is somewhat compressed relative to that of pentacene-h_{14}. The greek letters label the symmetry-equivalent carbon positions where a ^{13}C nucleus is located or to which a ^{1}H is bound (see Fig. 6). For the $\gamma-^1$H and $\varepsilon-^1$H satellites, the assignment could readily be verified through FDMR (see Sec. III B). The appearance of two ε satellites, labeled with the subscripts 1 and 2, is due to the lowering of the molecular symmetry caused by the embedding in the crystal sites which have inversion symmetry[19] (point group S_2). Instead of four D_{2h} symmetry-equivalent ε positions, two pairs of equivalent, diametrically opposite ε positions remain. A similar splitting is expected for the other groups of symmetry-equivalent positions apart from the two γ positions.

The identity of the other satellite bands (labeled β_2, β_1, and α_2) is somewhat ambiguous. It is obvious that they must

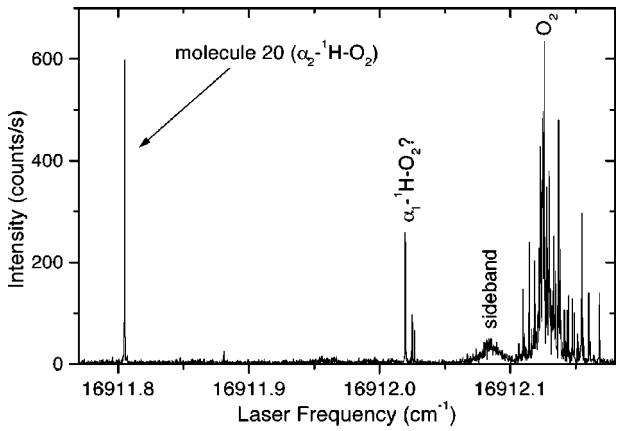

FIG. 5. In-focus excitation spectrum around the O_2 site. The smooth sideband is due to spectrally diffusing molecules. The three slightly redshifted molecules probably belong to the α_1-^1H species. The spectrum was recorded at low excitation power so as to minimize power broadening.

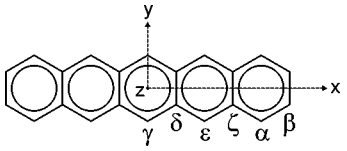

FIG. 6. The molecular structure of pentacene, $C_{22}H_{14}$, the greek letters label the-six symmetry-inequivalent carbon positions.

be due to isotopomers with a ^{1}H at one of the two remaining bonding positions, α and β. However based on FDMR spectra, no definitive assignment could be made. One would expect two pairs of split bands, one pair for α the other for β. Only three bands are observed. A possible interpretation is that for one pair the site distortion accidentally results in exactly the same isotope shift. However a more likely interpretation is that one of the bands is hidden under the flank or sideband of the main all-deutero band. This interpretation is supported by an observed excess occurrence of single molecules at a shift of roughly -0.11 cm^{-1} relative to the main all-deutero bands (see for example Fig. 5). Molecules 4 and 19 were selected at such a small shift.

Since a large splitting of a pair of bands of one isotopomeric species is unlikely, the two most redshifted bands can be assumed to correspond to one species, and the two least redshifted bands (one of which is hidden) to the other species. The assignment of β to the former and α to the latter is based on quantum-chemical calculations (see Table IV). This assignment is somewhat tentative given the moderate discrepancy between theory and experiment. The isotope shifts and assignments of the bands are summarized in Table I.

The intensities of the bands reflect the prevalence of the corresponding isotopomeric species. However the ensemble spectra were measured at an excitation intensity close to saturation so that the intersystem crossing rates particular to a species might also influence the observed intensity. For the ^{13}C isotopomer bands, the intensities were shown to be consistent with the prevalence of the isotopomers as calculated from the 1.1% ^{13}C natural abundance.[8] The ^{1}H impurities result from incomplete deuteration. Since the probability of ^{1}H–^{2}H exchange depends on the bonding position, the relatively large intensity of the $\gamma-^1$H bands need not be surprising. What does surprise is that the prevalences of isotopomers with multiple ^{1}H's, as judged from the intensities of the corresponding bands (see Fig. 1), are considerably higher than one expects given the probabilities of finding a ^{1}H in particular positions as determined from the intensity of the singly substituted bands. This might indicate that not all pentacene molecules had the same chances for exchange during deuteration. Alternatively it might be that there are large changes in the intersystem crossing rates between isotopic isomers. These considerations in part motivated us to study the intersystem crossing of these isotopomers.

B. Fluorescence-detected magnetic resonance

In previous work we have shown that the fluorescence-detected magnetic-resonance (FDMR) spectrum of the triplet state of a single pentacene molecule can serve to probe its isotopic composition.[8,20] Briefly, the nuclei present in the molecule may have a hyperfine and quadrupole interaction and influence the shape of the magnetic-resonance spectrum. The strength of the hyperfine interaction depends on the distribution of the triplet-spin density over the molecule which is known for pentacene[21] and thus allows a correlation between line shape and the presence and position of nuclei carrying a large magnetic moment (^{13}C and ^{1}H).

The lowest triplet state T_1 is populated after ISC from

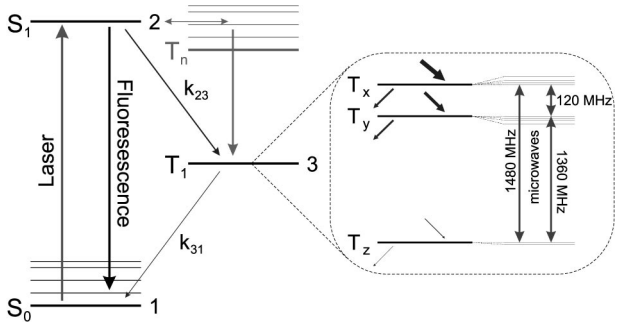

FIG. 7. Level scheme of pentacene in zero magnetic field. As indicated in the blowup to the right the lowest triplet state T_1 is split into three sublevels with different kinetics and hyperfine splitting. The two-way arrows connecting the sublevels indicate the possible microwave induced transitions. As indicated in grey, vibrational levels of a higher triplet T_n intermediate in the ISC from S_1 (see Sec. V).

S_1. As depicted in Fig. 7, hyperfine and quadrupole interactions cause a slight additional splitting of the three T_1 sublevels so that transitions between these sublevels established by means of applied microwaves will be broadened accordingly. As a specific example consider the FDMR spectrum shown in Fig. 8. The microwave frequency was scanned over the T_y-T_z and T_x-T_z sublevel transitions while saturating the S_0-S_1 transition using laser light. When inducing the T_y-T_z or T_x-T_z transition, the molecule will spend more time in the triplet state. Its time-average fluorescence decreases which allows the detection of the transition. The hyperfine broadening apparent in Fig. 8 can be used to confirm that molecule 18 contains ^{13}C nuclei at both γ positions (see Fig. 6). We will forego a discussion of the quantitative analysis which was performed using the method detailed in previous work.[8] Qualitatively, the sharp onset of each transition corresponds to an orientation of the two equivalent ^{13}C nuclear spins such that their hyperfine interactions cancel. The broad sideband of each transition corresponds to the case where the hyperfine interactions enhance each other.

The T_x-T_z transition rate depends on the projection of the microwave **B** field on the molecular y axis. Consequently, the intensities of spectra recorded for molecules be-

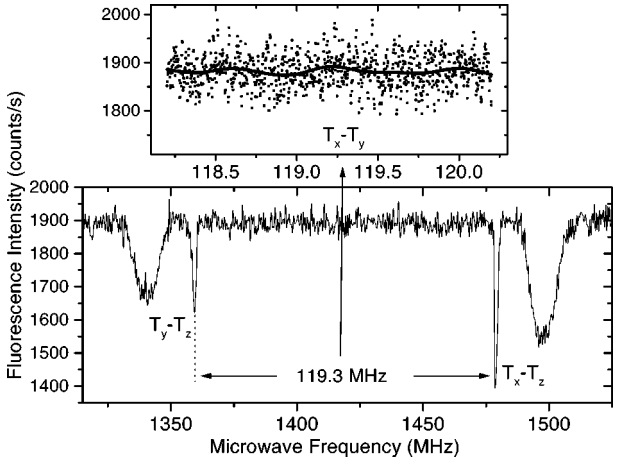

FIG. 8. FDMR spectrum of $\gamma\gamma^{13}$C–O$_2$ molecule 18. The hyperfine-split T_y-T_z and T_x-T_z transitions show up as a decrease in fluorescence. The T_x-T_y transition (inset) at 119.3 MHz could not be detected.

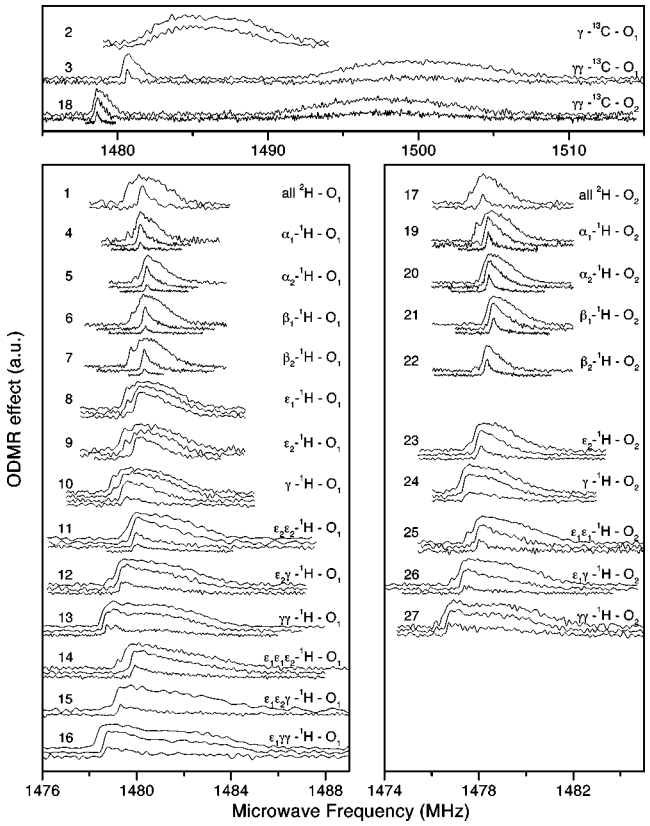

FIG. 9. Hyperfine-broadened FDMR lines of the T_x-T_z transition for the molecules studied. Each molecule was examined at a couple of microwave powers. The vertical scale is proportional to the FDMR effect which typically approached -30% at high microwave power.

longing to different sites or selected from different crystals are not mutually comparable even when the same microwave power has been used. For this reason we recorded FDMR spectra of each molecule at a couple of microwave powers so that the low to high power dependence could be extrapolated. The power dependence of the line shapes is due to a complicated mix of saturation effects. Also, at high power, quadrupole-induced $\Delta M_I \neq 0$ sidebands become visible though, remarkably, their appearance varies strongly from molecule to molecule. For the present discussion it suffices to note that the low power line shape is most representative of the hyperfine broadening.

An overview of the recorded FDMR line shapes for all examined molecules is given in Fig. 9. The line shapes are consistent with the assignment based on their optical transition frequency. Owing to the relatively high ε and γ spin density, the identity of molecules with ε or γ substitutions could be fully verified. In spite of averaging for a relatively long time at a high spectral resolution, a similar full verification proved impossible for molecules 4–7 and 19–22. Given their narrow line shapes it is clear that these molecules indeed do not have a ^{1}H in either the ε or γ positions but the small differences within each set of spectra did not allow for discrimination between the $\alpha-{}^1$H and $\beta-{}^1$H species.

The zero-field splitting as evident from the T_x-T_z transition frequency allowed molecules to be quickly classified as belonging to either the O_1 or O_2 site. As seen in Fig. 9 the

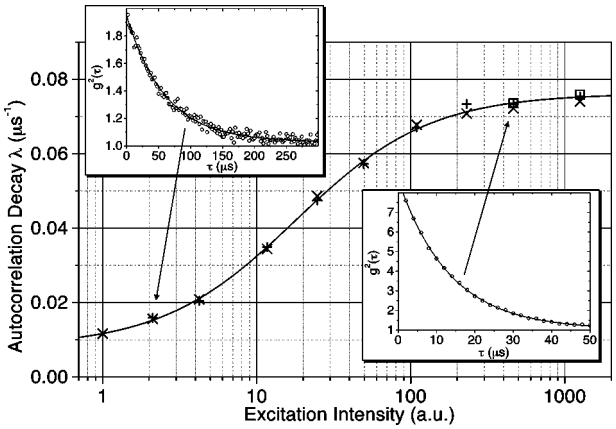

FIG. 10. Intensity dependence of the autocorrelation decay for $\gamma\gamma^{13}C-O_2$ molecule 18. The insets show the autocorrelation traces and exponential fits for two excitation intensities.

transition frequency is, on average, 2 MHz higher for the O_1 site. The variation in zero-field splitting for molecules belonging to the same site is relatively small (on the order of a few hundred kHz).

IV. RESULTS

The intersystem crossing rates of single pentacene molecules have been obtained by recording the autocorrelation of their fluorescence intensity as a function of the excitation intensity. The intensity autocorrelation function is defined as

$$g^2(\tau)=\langle I(t)I(t+\tau)\rangle/\langle I(t)\rangle^2, \tag{1}$$

where the angular brackets denote an average over time *t*. It can be measured by building a histogram counting the number of detected photon pairs separated by various τ times. By assuming a three-level system with level 1 the ground state S_0, level 2 the first excited singlet state S_1 and level 3 the lowest triplet state T_1 (see Fig. 7) Bernard *et al.*[5] showed that at intermediate time scales $(0.1\,\mu s<\tau<100\,\mu s$ for pentacene/*p*-terphenyl) $g^2(\tau)$ is well approximated by a single exponential

$$g^2(\tau)=1+C\exp(-\lambda\tau) \tag{2}$$

where

$$\lambda=k_{31}+\frac{k_{31}I/I_s}{1+2(k_{31}/k_{23})I/I_s}, \tag{3}$$

with I the excitation intensity, I_s the saturation intensity, k_{23} the intersystem crossing rate to the triplet state, and k_{31} the decay rate from the triplet to the ground state. Clearly, the correlation decay rate λ can be determined by fitting a single exponential to a recorded autocorrelation trace. By recording autocorrelation traces at a series of excitation intensities and determining λ for each intensity, a series of points is obtained to which Eq. (3) can be fit. Such a fit provides values for I_s, k_{23}, and k_{31}. Figure 10 shows an example fit together with a couple of the constituent autocorrelation traces.

By now one might wonder why a method based on treating the triplet as a single level is at all applicable. After all, the triplet T_1 state has three sublevels T_x, T_y, and T_z with

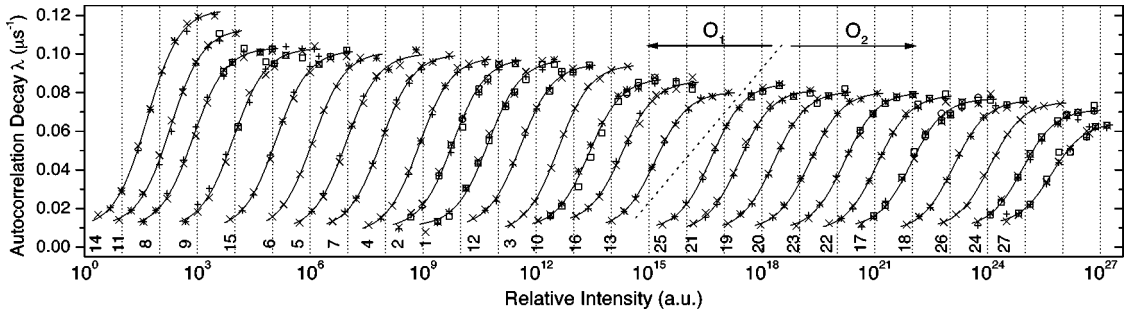

FIG. 11. Autocorrelation decay data and corresponding fits for all examined molecules. The crosses, plusses, circles, and squares discriminate repeated measurements at the same excitation intensity. The curves are mutually offset along the intensity axis to avoid overlap.

mutually differing populating and decay rates. For a complete description of the kinetic parameters a five instead of a three-level model is needed. Indeed, Brown *et al.* have performed such a complete analysis.[22] It turns out that the three-level model works well for the present purposes because the populating rate of the T_z sublevel is much smaller than that of the T_x and T_y levels which have nearly identical lifetimes as evident from the fact that the T_x-T_y transition was not detectable in spite of markedly different T_x and T_y populating rates (see Fig. 8). With no microwaves applied, the relatively long-lived T_z only slightly perturbs the monoexponential shape of the autocorrelation. Thus the described method determines the total intersystem crossing rate k_{23} as well as a triplet decay rate k_{31} that applies to both T_x and T_y but not T_z.

An overview of the autocorrelation data and corresponding fits for all examined molecules is given in Fig. 11. The kinetic parameters as determined through the fits are listed in Table II together with the site and isotopomer species. A subset of the isotopomers examined for the O_1 site were examined for the O_2 site so as to discriminate site dependent effects and gauge the reproducibility of any isotopomer dependence. To assist in the interpretation the change in intersystem crossing Δk_{23} relative to the perdeuterated species of each site is also tabulated.

V. DISCUSSION

The kinetic parameters summarized in Table II reveal that the triplet lifetimes ($\tau_{31}=k_{31}^{-1}$) are mostly clustered near an average of 110 μs for both the O_1 and O_2 site. No clear isotopomer dependent trend can be discerned within the rather limited precision. In contrast, the $S_1\rightarrow T_1$ intersystem crossing rate k_{23} does differ significantly between the sites. O_1 molecules have, on average, a 29% higher k_{23} rate as compared to O_2 molecules of the same isotopic composition. In addition, there is a marked dependence of k_{23} on isotopic composition that reproduces for both sites. A single ^{1}H in the ε, α, or β position causes an increase in ISC of roughly 5%–8%. In contrast, a ^{1}H in the γ position decreases k_{23} by about 10%. Only for the α position is a significant discrepancy between molecules from either distortion-split band (α_1 and α_2) observed. When examining the results for molecules containing multiple ^{1}H, a trend in Δk_{23} becomes evident as made explicit in Table III. Clearly k_{23} decreases with the number of γ ^{1}H's and increases with the number of ε ^{1}H in a way that is approximately additive.

Changes in the isotopic composition of a molecule have a marked influence on vibrational frequencies. Consequently the observed dependence of the $S_1\rightarrow T_1$ ISC rate k_{23} on the isotopic composition most probably relates to changes in vibrational frequencies between isotopic isomers. When substituting a ^{1}H for a ^{2}H the mass of the involved atom is halved which causes all associated normal-mode frequencies (particularly those of the C–H stretch, in-plane rock and out-of-plane wag modes) to increase in a way that is very similar for the various substitution positions. Yet k_{23} is found to decrease for a γ substitution and to increase for an ε substitu-

TABLE II. Triplet kinetics for all examined molecules.

Molecule No.	Site	Type	k_{23} (kHz)	Δk_{23} (kHz)	τ_{31} (μs)
1	O_1	all-^{2}H	173.6±4.0	0	94±17
2	O_1	γ-^{13}C	177.4±8.8	+3.8	106±49
3	O_1	γ-^{13}C	175.3±1.9	+1.7	139±13
4	O_1	α_1-^{1}H	183.3±2.1	+9.7	143±16
5	O_1	α_2-^{1}H	184.2±3.0	+10.6	119±18
6	O_1	β_1-^{1}H	186.4±3.0	+12.8	120±19
7	O_1	β_2-^{1}H	182.8±1.7	+9.2	113±8
8	O_1	ε_1-^{1}H	187.6±2.2	+14.0	103±9
9	O_1	ε_2-^{1}H	187.0±3.1	+13.4	102±14
10	O_1	γ-^{1}H	155.9±2.8	−17.7	102±12
11	O_1	$\varepsilon_2\varepsilon_2$-^{1}H	205.7±2.6	+32.1	94±9
12	O_1	$\varepsilon_1\gamma$-^{1}H	170.2±2.1	−3.4	100±8
13	O_1	$\gamma\gamma$-^{1}H	142.6±1.6	−31.0	108±7
14	O_1	$\varepsilon_1\varepsilon_1\varepsilon_2$-^{1}H	227.3±2.1	+53.7	103±9
15	O_1	$\varepsilon_1\varepsilon_2\gamma$-^{1}H	187.0±2.4	+13.4	114±13
16	O_1	$\varepsilon_1\gamma\gamma$-^{1}H	148.3±3.0	−25.3	82±9
17	O_2	all-^{2}H	134.7±4.3	0	101±20
18	O_2	$\gamma\gamma$-^{13}C	136.7±1.7	+2.0	124±9
19	O_2	α_1-^{1}H	145.4±1.5	+10.7	121±8
20	O_2	α_2-^{1}H	143.6±1.3	+8.9	112±5
21	O_2	β_1-^{1}H	147.9±1.7	+13.2	128±10
22	O_2	β_2-^{1}H	141.8±1.8	+7.1	124±10
23	O_2	ε_2-^{1}H	143.5±1.5	+8.8	115±7
24	O_2	γ-^{1}H	123.8±1.9	−10.9	104±8
25	O_2	$\varepsilon_1\varepsilon_1$-^{1}H	152.6±1.6	+17.9	114±8
26	O_2	$\varepsilon_1\gamma$-^{1}H	132.2±1.8	−2.5	107±8
27	O_2	$\gamma\gamma$-^{1}H	106.9±2.5	−27.8	89±8

TABLE III. The change in ISC upon γ and/or ε ^{1}H substitution relative to the perdeuterated case. An additive trend is apparent.

	Δk_{23} (kHz)		
O_1		γ	$\gamma\gamma$
	0	−17.7	−31.0
ε	+13.7	−3.4	−25.3
$\varepsilon\varepsilon$	+32.1	+13.4	
$\varepsilon\varepsilon\varepsilon$	+53.7		
O_2		γ	$\gamma\gamma$
	0	−10.9	−27.8
ε	+8.8	−2.5	
$\varepsilon\varepsilon$	+17.9		

TABLE IV. Calculated S_0-S_1 and T_3-S_1 isotope shifts relative to the perdeuterated case. The average of the corresponding experimentally determined S_0-S_1 shifts (see Table I) is listed for comparison.

	Isotope shift (cm^{-1})		
Isotopomer	Experimental S_0-S_1	Calculated S_0-S_1	Calculated T_3-S_1
γ-^{1}H	−4.16	−6.75	7.13
ε-^{1}H	−3.35	−5.04	−4.77
β-^{1}H	−0.89	0.68	5.36
α-^{1}H	−0.32	1.02	14.29

tion. This specificity to the substitution position suggests a dependence on the electronic structure.

There exists a molecular property that does depend both on differences in electronic structure between two states as well as on changes in vibrational frequencies upon isotope substitution in a way that is additive; an isotope shift. Isotope shifts result from the zero-point energy depending on the electronic state as well as on the isotopic composition which causes slight shifts in the energy difference between two electronic states for various isotopomers. The sign of a shift depends on whether the bonding strengthens or weakens at the substitution position in going from one electronic state to the other. The observed changes in ISC might therefore be elucidated if k_{23} can be shown to correlate with an isotope shift.

To explain experiments on anthracene in supersonic jets, Amirav *et al.*[23] proposed a coupling scheme in which the ISC from S_1 is intermediated, through spin-orbit coupling and subsequent internal conversion, by vibrational levels of an nth triplet state $\{T_n^k\}$ (see Fig. 7). They derived the following expression for the resulting contribution to the ISC rate:

$$\sum_k \frac{V_{SO}^2(k)\Delta_k}{[E(S_1)-E(T_n^k)]^2+(\Delta_k/2)^2}, \tag{4}$$

where k sums over the vibrational levels, $V_{SO}(k)$ is the $S_1-T_n^k$ spin-orbit coupling (SOC) matrix element and Δ_k is the decay width of T_n^k. Direct evidence for the same mechanism being operational in pentacene was found by Corval *et al.*[15] By shifting triplet sublevels using a strong magnetic field, they observed a T_n^k sublevel crossing with S_1 for pentacene in benzoic acid. Semiempirical CNDOM calculations implicated T_3 as the only plausible candidate.[15]

Isotope shifts of the energy difference between S_1 and T_3 modulate the denominator of Eq. (4), and thereby change the ISC rate. The same holds for the particular frequencies of the vibrational levels T_3^k close to S_1 that make a dominant contribution. It is therefore, in principle, possible that the observed changes in k_{23} depend on isotope shifts via the above mechanism, but a quantitative verification requires a means to determine these isotope shifts as well as an analysis of vibrational frequencies.

As opposed to the S_0-S_1 isotope shifts, the T_3-S_1 isotope shifts are not experimentally accessible and therefore require quantum-chemical calculations. We performed CI-singles *ab initio* calculations with the largest practical basis set using GAUSSIAN 94.[24] A full account of these and normal coordinate calculations, as well as a discussion of isotope shifts and intersystem crossing from a somewhat more general perspective will be given in a forthcoming paper.[25] Here we limit ourselves to summarizing the results of direct relevance to explaining the experimental data.

Given the size of pentacene the calculations are necessarily limited in precision. Still, it proves possible to obtain a rough, qualitative description of the ^{1}H-substitution isotope shifts as shown for the S_0-S_1 shifts in Table IV. It should be noted that part of the discrepancy is due to the calculations not accounting for the effects of the host matrix which are not negligible as evident from the splitting of the isotope-shifted bands observed in the ensemble excitation spectra.

The calculated T_3-S_1 isotope shifts are also listed in Table IV. The shifts for γ and ε are indeed opposite and their relative magnitude is similar to the relative magnitude of the corresponding changes in ISC (see Table III) which corroborates the hypothesis that T_3 and S_1 isotope shifts modulate k_{23}. A normal coordinate analysis using the force field described in Ref. 26, shows that there are indeed a few out-of-plane modes [which, being out-of-plane, have large $V_{SO}(k)$] that hardly shift for substitution in the ε and γ position, in particular the C$-^2$H out-of-plane modes in which adjacent α and β ^{2}H move in and out of phase. A near resonance of S_1 with one of these modes causing a dominant contribution to the ISC as per Eq. (4) would allow the isotope shift to modulate the intersystem crossing for γ and ε substitution and would explain the lack of correlation of Δk_{23} with the ^{1}H shifts calculated for α and β.

If these γ and ε isotope shifts indeed modulate k_{23} by some 10% per substitution, Eq. (4) implies that S_1 should be detuned from the dominant T_3 vibrational level(s) by a few tens of wave numbers. An S_1-T_3 solvent shift of similar magnitude is therefore sufficient to bring S_1 into close resonance with these or other vibrational levels thereby vastly enhancing ISC. This might explain the two orders of magnitude larger ISC for the O_3 and O_4 sites (at 17 031.7 and 17 091.0 cm^{-1}) as compared to the O_1 and O_2 sites (at 16 908.5 and 16 912.2 cm^{-1}) of deuterated pentacene in *p*-terphenyl[12,13] as the S_1-S_0 and S_1-T_3 solvent shifts are likely to be correlated.

VI. CONCLUSION

We have demonstrated the feasibility of studying a large set of isotopic isomers not through synthesis and ensemble spectroscopy, but rather through the selection, by means of excitation spectroscopy and fluorescence-detected magnetic resonance, of single molecules belonging to specific isotopomer species present as an accidental impurity. The triplet kinetics of pentacene molecules was determined through fluorescence autocorrelation. A marked trend in the $S_1 \rightarrow T_1$ intersystem crossing of pentacene for various isotopomers was observed. We attribute this trend to the modulation of a near resonance between the first excited singlet state S_1 and vibrational levels of a higher lying triplet T_3 by isotope shifts of these electronic states, an interpretation corroborated by quantum-chemical calculations.

ACKNOWLEDGMENTS

The authors are indebted to Professor H. Zimmerman and Professor H. M. Vieth for kindly providing the deuterated pentacene used in the experiments and to Dr. A. Krüger for providing the zone-refined *p*-terphenyl from which the crystal flakes were grown. We wish to thank Dr. H. C. Fleischhauer for sharing the pentacene force field used for normal coordinate analysis. The quantum-chemical calculations were performed in cooperation with Dr. M. C. van Hemert. This work forms part of the research program of the ''Stichting voor Fundamenteel Onderzoek der Materie'' (FOM) with financial aid from the ''Nederlandse Organisatie voor Wetenschappelijk Onderzoek'' (NWO). J. Köhler is a Heisenberg Fellow of the ''Deutsche Forschungsgemeinschaft'' (DFG).

[1] W. E. Moerner and T. Basché, Angew. Chem. Int. Ed. Engl. **32**, 457 (1993).
[2] M. Orrit, J. Bernard, and R. I. Personov, J. Phys. Chem. **97**, 10256 (1993).
[3] W. E. Moerner, Science **265**, 46 (1994).
[4] L. Kador, Phys. Status Solidi B **189**, 11 (1995).
[5] J. Bernard, L. Fleury, H. Talon, and M. Orrit, J. Chem. Phys. **98**, 850 (1993).
[6] M. Vogel, A. Gruber, J. Wrachtrup, and C. von Borczyskowski, J. Phys. Chem. **99**, 14915 (1995).
[7] A. C. J. Brouwer, E. J. J. Groenen, and J. Schmidt, Phys. Rev. Lett. **80**, 3944 (1998).
[8] A. C. J. Brouwer, J. Köhler, E. J. J. Groenen, and J. Schmidt, J. Chem. Phys. **105**, 2212 (1996).
[9] J. Köhler, A. C. J. Brouwer, E. J. J. Groenen, and J. Schmidt, J. Am. Chem. Soc. **120**, 1900 (1998).
[10] W. E. Moerner and L. Kador, Phys. Rev. Lett. **62**, 2535 (1989).
[11] M. Orrit and J. Bernard, Phys. Rev. Lett. **65**, 2716 (1990).
[12] H. de Vries and D. A. Wiersma, J. Chem. Phys. **70**, 5807 (1979).
[13] F. G. Patterson, H. W. H. Lee, W. L. Wilson, and M. D. Fayer, Chem. Phys. **84**, 51 (1984).
[14] J. O. Williams, A. C. Jones, and M. J. Davies, J. Chem. Soc., Faraday Trans. 2 **79**, 263 (1983).
[15] A. Corval, C. Kryschi, S. Astilean, and H. P. Trommsdorff, J. Phys. Chem. **98**, 7376 (1994).
[16] S. Gerstenkorn and P. Luc, *Atlas du Spectre d'Absorption de la Molécule d'Iode* (Editions du CNRS, Paris, 1978).
[17] S. Gerstenkorn and P. Luc, Rev. Phys. Appl. **14**, 791 (1979).
[18] T. Basché, S. Kummer, and C. Bräuchle, Chem. Phys. Lett. **225**, 116 (1994).
[19] J. L. Baudour, Y. Delugeard, and H. Cailleau, Acta Crystallogr., Sect. B: Struct. Crystallogr. Cryst. Chem. **32**, 150 (1976).
[20] J. Köhler, A. C. J. Brouwer, E. J. J. Groenen, and J. Schmidt, Science **268**, 1457 (1995).
[21] T. S. Lin, J. L. Ong, D. J. Sloop, and H. L. Yu, in *Pulsed EPR: A New Field of Applications*, edited by C. Keijzers, E. Reijerse, and J. Schmidt (North-Holland, Amsterdam, 1989), p. 191.
[22] R. Brown, J. Wrachtrup, M. Orrit, J. Bernard, and C. von Borczyskowski, J. Chem. Phys. **100**, 7182 (1994).
[23] A. Amirav, M. Sonnenschein, and J. Jortner, Chem. Phys. Lett. **100**, 488 (1983).
[24] M. J. Frisch, G. W. Trucks, H. B. Schlegel, P. M. W. Gill, B. G. Johnson, M. A. Robb, J. R. Cheeseman, T. Keith, G. A. Petersson, J. A. Montgomery, K. Raghavachari, M. A. Al-Laham, V. G. Zakrzewski, J. V. Ortiz, J. B. Foresman, J. Cioslowski, B. B. Stefanov, A. Nanayakkara, M. Challacombe, C. Y. Peng, P. Y. Ayala, W. Chen, M. W. Wong, J. L. Andres, E. S. Replogle, R. Gomperts, R. L. Martin, D. J. Fox, J. S. Binkley, D. J. Defrees, J. Baker, J. P. Stewart, M. Head-Gordon, C. Gonzalez, and J. A. Pople, *Gaussian 94, Revision D.4* (Gaussian, Pittsburgh, PA, 1995).
[25] A. C. J. Brouwer, M. C. van Hemert, E. J. J. Groenen, and J. Schmidt, J. Phys. Chem. (submitted).
[26] H. C. Fleischhauer, Ph.D. thesis, Heinrich-Heine-Universität Düsseldorf, 1992.